ADVANCED MATERIALS TECHNOLOGIES

# Supporting Information

for *Adv. Mater. Technol.,* DOI: 10.1002/admt.202201640

## Flow Casting Soft Shells with Geometrical Complexity and Multifunctionality

*Dongliang Fan, Yuxuan Liao, Wenyu Wu, Ping Zhang, Xin Yang, Renjie Zhu, Yifei Wang, Canhui Yang, and Hongqiang Wang**

# Supporting Information

**Flow casting soft shells with geometrical complexity and multifunctionality**

*Dongliang Fan, Yuxuan Liao, Wenyu Wu, Ping Zhang, Xin Yang, Renjie Zhu, Yifei Wang, Canhui Yang, Hongqiang Wang**

**Corresponding author. Email: wanghq6@sustech.edu.cn*

This PDF file includes:

Supplementary Text
Figures S1 to S8
Table S1
Legends for Movies S1 to S5

Other Supplementary Materials for this manuscript include the following:

Movies S1 to S5

**Supporting Information Text**

## 1. Layer thickness control

### 1.1 Experimental characterization

After the Ecoflex 0050 precursor was stirred for 1 minute and vacuumed for 4 minutes, the precursor was injected into an acrylic tube (diameter: 4 mm, length: 10 cm). Once all the precursor was drained out of the tube (Figure 2A), the tube with the precursor layer was fixed horizontally and rotated along the axial direction. Then, a heat gun (working temperature: 250 ℃) was used to heat the tube at a 2 cm distance to generate a quick curing process for the initial layer thickness obtaining. The relationship between the initial layer thickness of the precursor and the different positions is shown in Figure S1 in the supporting information. The initial thickness $h_i$ is governed by:

$$h_i = 0.41 - 0.41e^{-0.1z} \#(S1)$$

where z is the position. The viscosity measurement was conducted on a rheometer (Discovery HR 30, TA instruments) in dynamic mode at room temperature, and the applied strain was 0.1% with a frequency of 1 Hz. The Ecoflex 0050 precursor was stirred and vacuumed before pouring into a 20 mm stainless steel parallel plate. The test duration was 2500 s. The relationship between viscosity and time is shown in Figure S1 in the supporting information. The viscosity $\mu_t$ is controlled by:

$$\mu_t = 6.28441 + 1.05835e^{0.00145t} \#(S2)$$

where t is the waiting time.

### 1.2 Mathematical modeling

According to the Navier-Stokes equations, and assuming that the inertial force can be neglected near the wall:

$$g = -\frac{1}{\rho}\frac{\partial P}{\partial z} - \frac{\mu}{\rho}\frac{\partial^2 u}{\partial r^2} \#(S3)$$

where $P(z,t)$ is the vertical pressure, $u(r,z,t)$ is the vertical velocity, and $\mu$ represents the dynamic viscosity.

Following the assumption that there is no slip between the surface liquid and the wall, and one of the boundary conditions is:

$$u(0,z,t) = 0 \#(S4)$$

On the free surface of the liquid at $r = h(z,t)$, where $h(z,t)$ is the thickness of the liquid layer, the tangent stress must be zero, so the other boundary condition is:

$$\frac{\partial u(h,z,t)}{\partial r} = 0 \#(S5)$$

Ignoring the horizontal pressure on that free surface, the pressure inside the liquid must equal to the capillary pressure:

$$P = \frac{\sigma}{R} = \frac{\sigma}{\frac{\left[1+\left(\frac{\partial h}{\partial z}\right)^2\right]^{\frac{3}{2}}}{\frac{\partial^2 h}{\partial z^2}}} \approx \sigma\frac{\partial^2 h}{\partial z^2} \#(S6)$$

For equation (S3), do the integral operation and apply the boundary conditions, we obtain:

$$u = -\frac{\rho}{\mu}\left(g + \sigma\frac{\partial^3 h}{\partial z^3}\right)\left(\frac{1}{2}r^2 - h\cdot r\right) \#(S7)$$

According to the mass conservation, hence:

$$\frac{\partial h}{\partial t} + \frac{\partial Q}{\partial z} = 0 \#(S8)$$

$$Q = \int_0^h u dr \#(S9)$$

We finally obtain the partial differential equation (PDE) with independent variables position $z$ and waiting time $t$:

$$\frac{\partial h}{\partial t} + \frac{1}{\mu}\left[\frac{\sigma}{3}\cdot h^3\frac{\partial^4 h}{\partial z^4} + \sigma\cdot h^2\frac{\partial^3 h}{\partial z^3}\frac{\partial h}{\partial z} + \rho g\cdot h^2\frac{\partial h}{\partial z}\right] = 0 \#(S10)$$

Assuming that the depth of the fluid varies slowly along the substrate and that the effect of surface tension is negligible:

$$\frac{\partial h}{\partial t} + \frac{\rho g}{\mu}\cdot h^2\frac{\partial h}{\partial z} = 0 \#(S11)$$

### 1.3 Analytical solution

Assuming that $h(z,t) = T(t)Z(z)$, then equation (S11) can be rewritten as:

$$Z\frac{dT}{dt} + \frac{\rho g}{\mu}\cdot (ZT)^2\cdot T\frac{dZ}{dz} = 0 \#(S12)$$

Simplify it, and we obtain:

$$ZZ' = -\frac{T'}{T^3}\frac{\mu}{\rho g} \#(S13)$$

Do the integral operation, and we obtain:

$$Z = \sqrt{C_1 - \frac{2\mu}{\rho g}\frac{T'}{T^3}z} \#(S14)$$

where $C_1$ is the constant independent of z and t.

Since Z is the function independent of t, we get:

$$C_0 = \frac{2\mu}{\rho g}\frac{T'}{T^3} \#(S15)$$

where $C_0$ is the constant and independent of z and t.

Consider that viscosity varies with time in terms of $\mu = \mu_0 + \alpha e^{\beta t}$, in which the constants are obtained from equation (S2), then do the integral operation, and we obtain:

$$T = \sqrt{\frac{1}{-\frac{C_0 \rho g}{\beta \mu_0}\{\beta t - \ln[\mu_0 + \alpha e^{\beta t}]\} + C_2}} \#(S16)$$

where $C_2$ is the constant independent of z and t.

Hence, the layer thickness is governed by:

$$h(z,t) = T(t)Z(z) = \sqrt{\frac{C_1 - C_0 z}{-\frac{C_0 \rho g}{\beta \mu_0}\{\beta t - \ln[\mu_0 + \alpha e^{\beta t}]\} + C_2}} \#(S17)$$

Assuming that the initial thickness equation (S1) can be simplified as $h_i = \sqrt{\frac{0.35^2}{20}z}$, substitute it to equation (S17), we finally obtain:

$$h(z,t) = \sqrt{\frac{z}{\frac{\rho g}{\beta \mu_0}\{\beta t - \ln[\mu_0 + \alpha e^{\beta t}]\} + 163.3}} \#(S18)$$

**1.4 Numerical solution**

COMSOL Multiphysics 5.6 is used to calculate the numerical solution of equation (S11).

**1.5 Results and comparison**

In considering the errors of time and size measurement during the experiment, the final thickness is multiplied by a correction factor $k = 1.25$. The results and comparison are shown in Figure 2B, C.

**2. Characteristics of the demolding process**

Consider the peeling of a thin elastic film from the inner wall of a rigid tube of the type shown in Figure S3 in the supporting information. The inner diameter of the original tube is D, and the inner diameter of the coated tube is d. The elastic film has thickness $t = (D - d)/2$ and a cross-sectional area $A_c = \pi t(D - t)$. Upon peeling, the top end of the film (denoted as Region e) is clamped onto a loading cell and subject to an external load F with controlled displacement. Part of the region (denoted as Region a) detaches, deforms considerably, and is substantially under simple extension. The undetached region (denoted as Region b) is substantially undeformed. A transition region (denoted as Region c) exists in the neighborhood of the crack tip. The deformation states of both c and e are complicated. However, when the length of the detached region is sufficiently long compared to the inner diameter of the tube, the release of the elastic film from the tube reaches a steady state. At steady state, a small increase in the length of the detached region under constant external force, dc, increases the size of Region a, which is in a simple extension state, at the expense of the undeformed Region b, while leaving the deformation states in Region C and E unaltered. The increase in the volume of Region a at the expense of Region b is $A_c \cdot dc = \pi t(D - t) \cdot dc$. The deformation state of the materials in Region a is unaltered since it only depends on the external force F, which plateaus in a steady state. Assume that the displacement of the loading cell l increases by an amount of dl, and let the stretch of Region a be $\lambda$, then we have:

$$\left(\frac{\partial l}{\partial c}\right)_F = \lambda \#(S19)$$

The elastic energy U stored in the film is a function of c and l, $U(c, l)$. Therefore, the change in elastic energy dU, due to the change in the length of detached region dc and the overall displacement of loading cell dl, is given by:

$$dU = \left(\frac{\partial U}{\partial c}\right)_l dc + \left(\frac{\partial U}{\partial l}\right)_c dl \#(S20)$$

Note that $\left(\frac{\partial U}{\partial l}\right)_c = F$. Substituting it into equation (S19) yields:

$$\left(\frac{\partial U}{\partial c}\right)_l = \left(\frac{\partial U}{\partial c}\right)_F - F\lambda \#(S21)$$

An increase in the length of the detached region under constant external force, dc, transfers a volume in the undeformed state, $A_c \cdot dc$, to one in the simple extension state. The change in elastic energy dU is:

$$\left(\frac{\partial U}{\partial c}\right)_F = W(\lambda)A_c \#(S22)$$

Introducing the relation (S22) into (S21), we obtain:

$$\left(\frac{\partial U}{\partial c}\right)_l = W(\lambda)\pi(D-t) - F\lambda \#(S23)$$

The energy release rate is defined as:

$$G = \left.\frac{\partial U(c,l)}{\partial S}\right|_l \#(S24)$$

where S is the area of the detached region, $S = \pi Dc$, substitute equation (S23) into (S24), we get:

$$G = \frac{F\lambda}{\pi D} - \frac{t(D-t)}{D}W(\lambda) \#(S25)$$

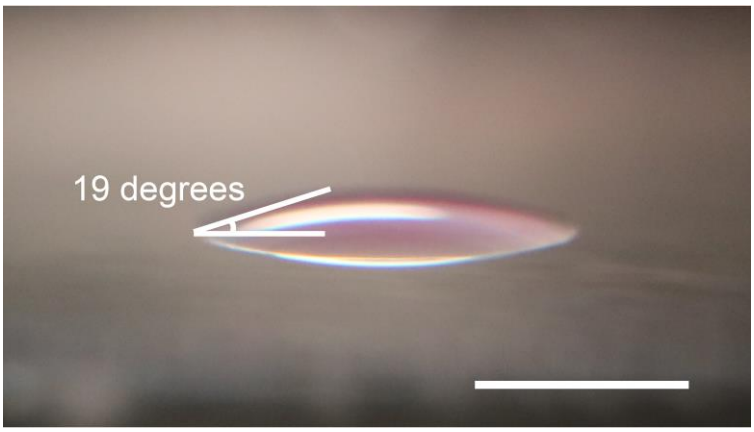


**Figure S1.** The contact angle of the elastomer precursor on an acrylic substrate. Scale bar, 1 mm.

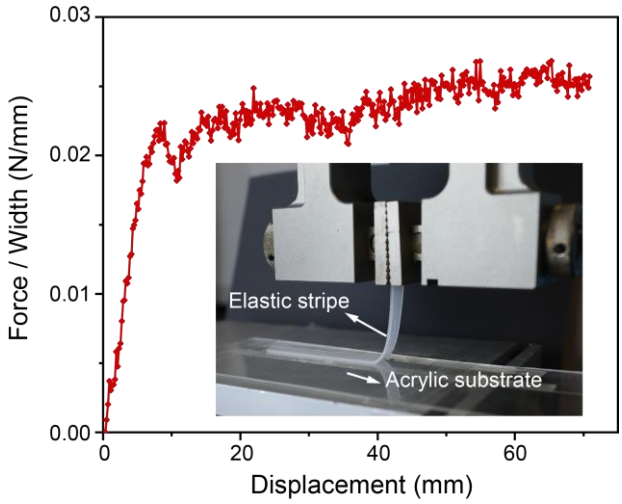


**Figure S2.** The adhesion strength measurement for the elastic strip on an acrylic substrate by a 90-degree peel test. The dimensions of the elastic strip: 10 cm in length, 1 cm in width, and 1 mm in thickness.

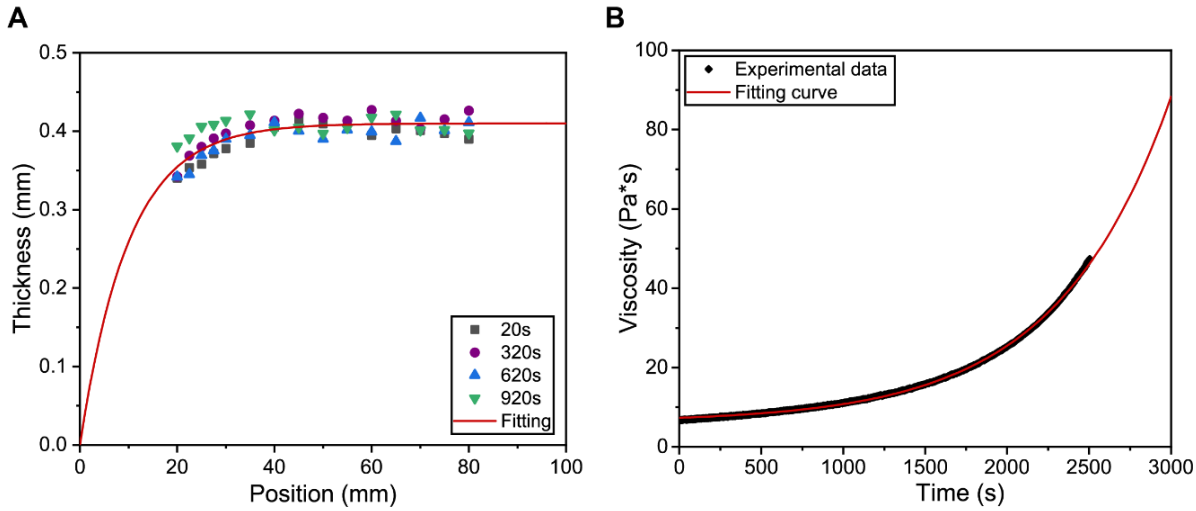


**Figure S3.** Layer thickness control. A) The initial thickness of precursor on the acrylic tube versus position. B) The relationship between viscosity and time.

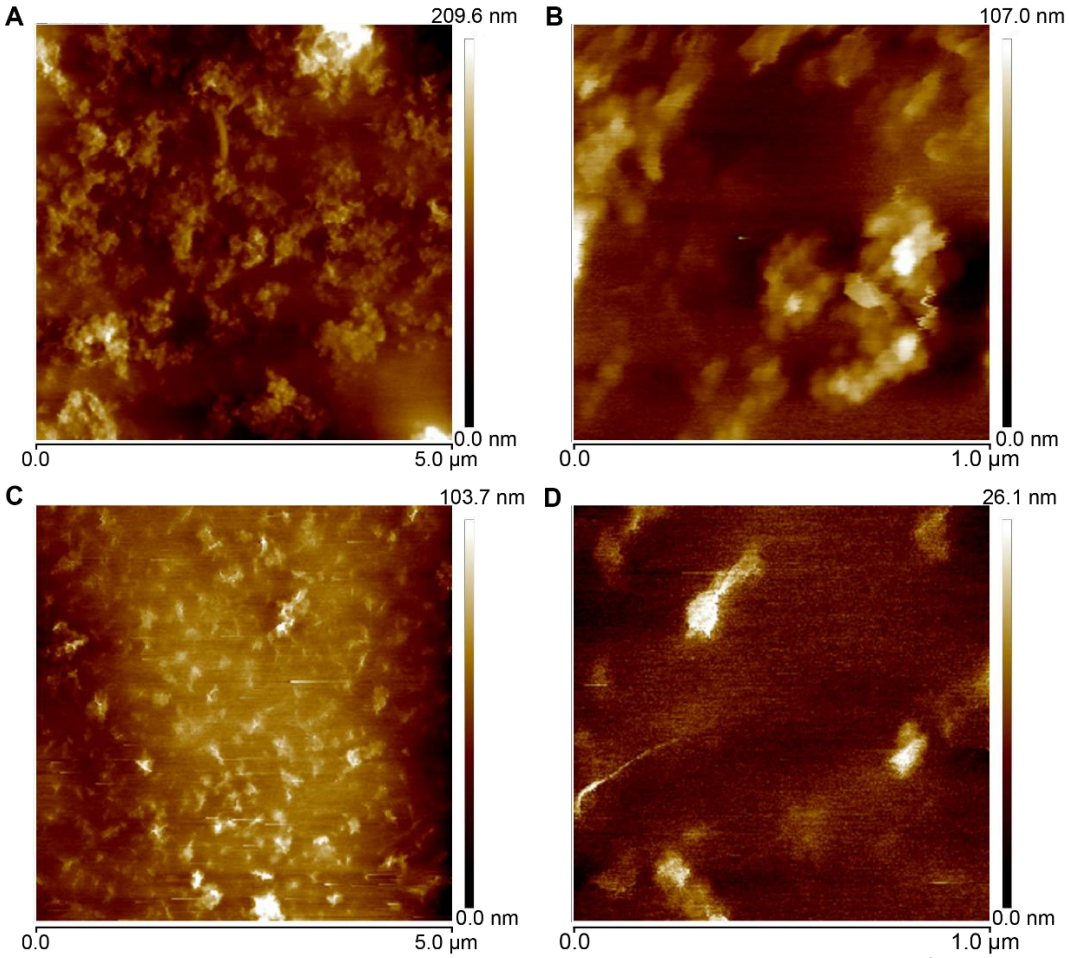


**Figure S4.** Surface roughness of the soft tube. A) An AFM scan image over a 25 µm$^2$ area and B) a 1 µm$^2$ area on an inner surface of the soft tube. C) An AFM scan image over a 25 µm$^2$ area and D) a 1 µm$^2$ area on an outer surface of the soft tube.

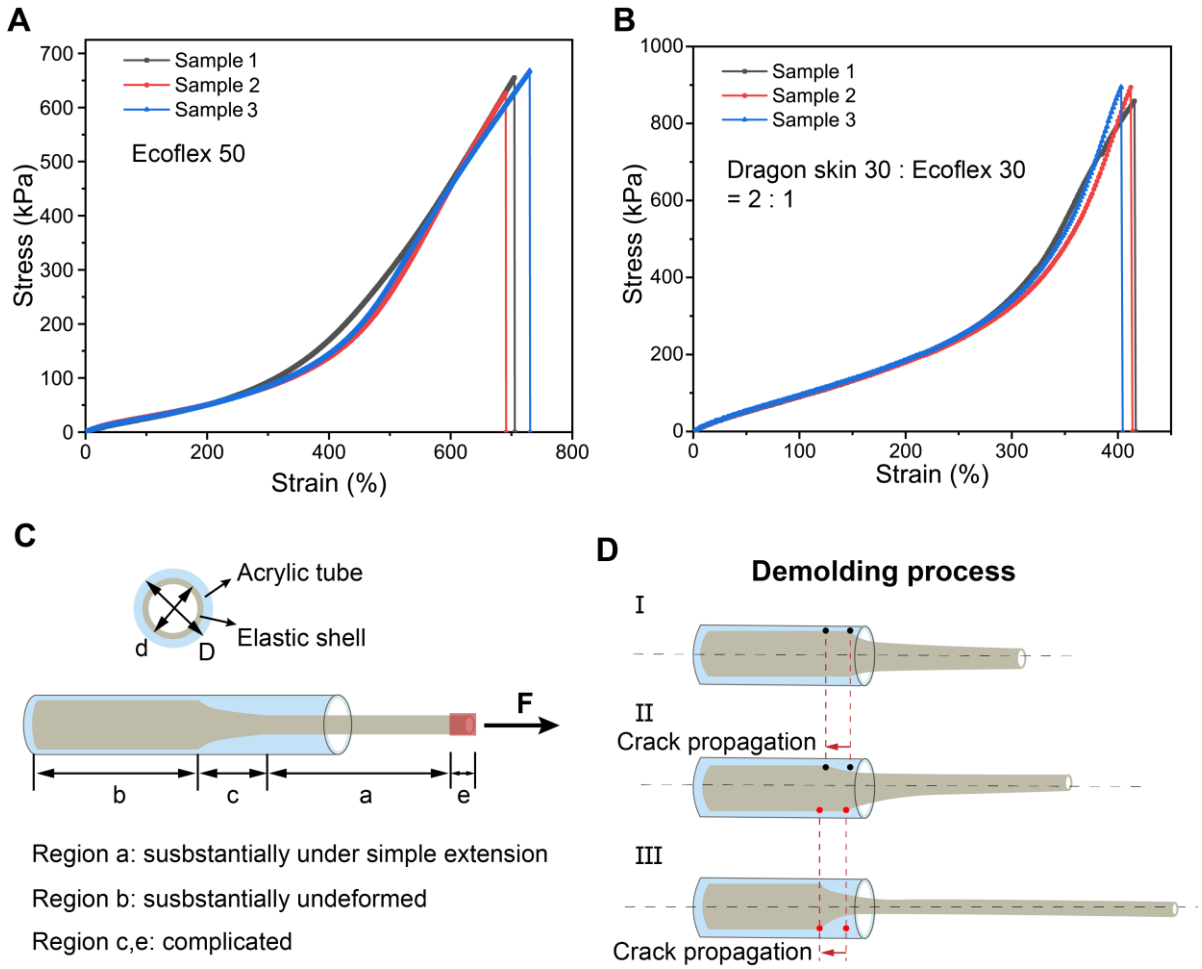


**Figure S5.** Mechanical characteristics of the elastic tubes. A) The stress-strain curve of Ecoflex 0050 tube with n=3 samples. B) The stress-strain curve of the mixture tube with 3 samples. C) Mechanics of peeling a thin elastic film from the inner wall of a rigid tube. The inner diameter of the original tube is D, and the inner diameter of the coated tube is d. During peeling, part of the elastic film is clamped by an external loading cell (Region e) and subject to an external force F. Region a is detached from the tube and is substantially under simple extension. The undetached Region b is substantially undeformed. A transition Region c, in which the crack tip is located, exists between a and b. The deformation states of both c and e are complicated in character. D) Schematic of stepwise demolding process. I) shows that the elastic shell exists a deviation from the center of the acrylic tube when a force applied. II) shows the top region of the elastic tube initiates demolding. III) shows the bottom region of the elastic tube initiates demolding.

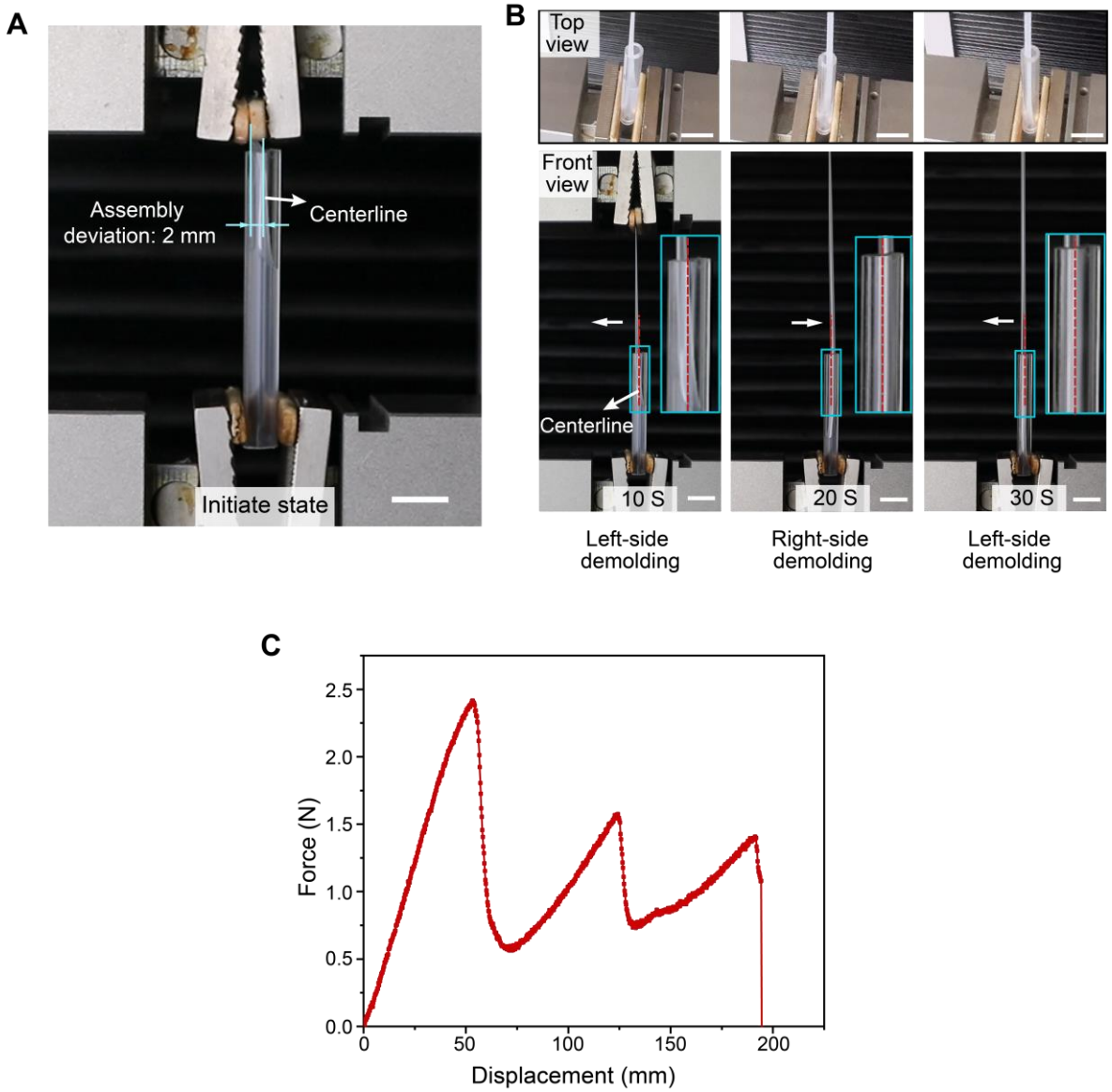


**Figure S6.** Effect of assembly deviation for the soft shell demoding process. A) Applying a 2 mm-deviation of the applied force to the experiment system. B) The discrete demolding process from two viewing angles. C) The force-displacement curve during the demolding process. Scale bars, 10 mm.

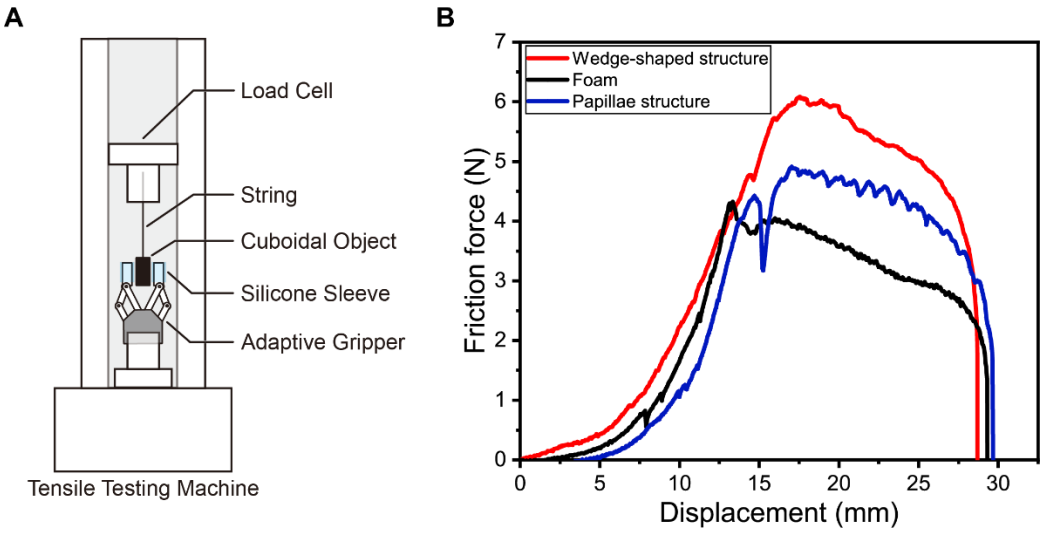


**Figure S7.** Friction tests of the soft sleeves. A) The schematic diagram of the setup for the friction tests. B) The friction force vs. displacement curve for all three structures with the same load (4 N).

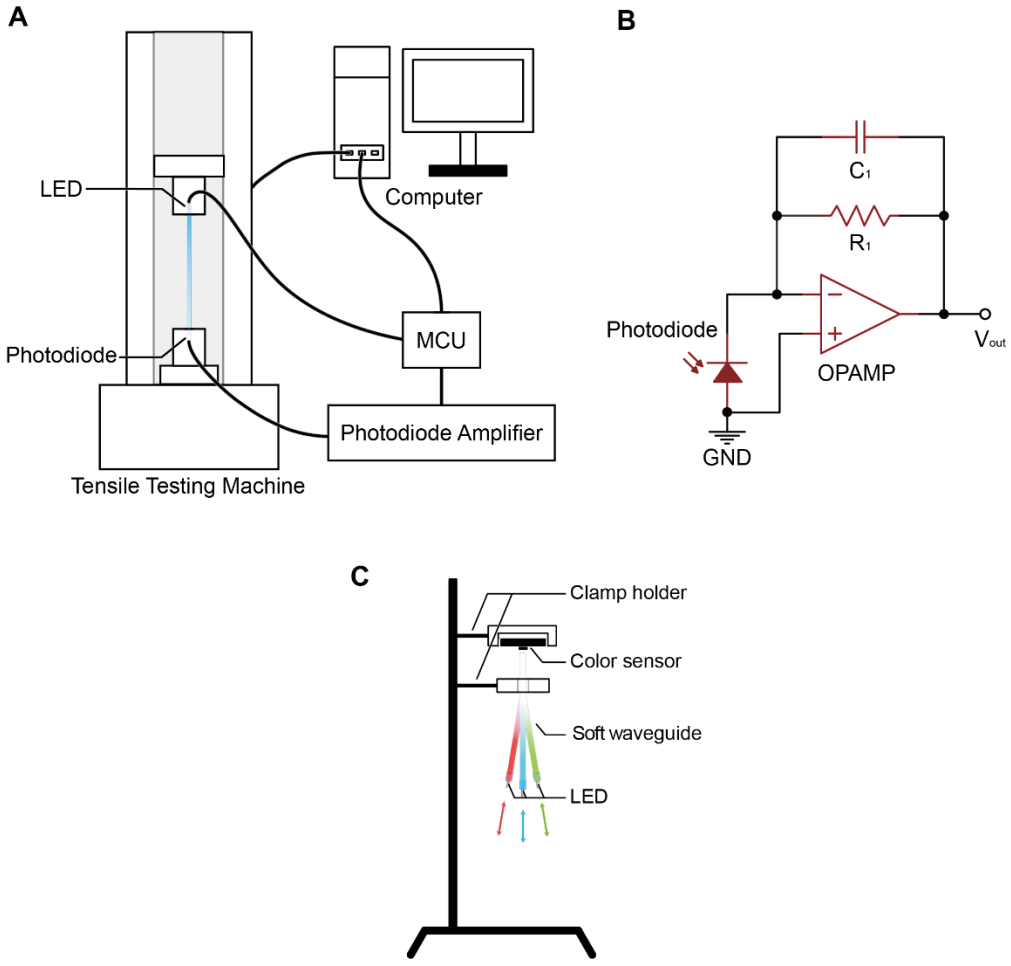


**Figure S8.** Setup for the soft optical waveguides test. A) The schematic diagram of the setup for the optical signal test during stretching. B) The circuit of the photodiode amplifier. C) The setup for the chromatic changes test. These three arrows with different colors display the stretching directions of the input branches.

**Table S1.** Comparisons of existing soft shell fabrication technologies

| Fabrication methods | **Mold casting**[19, 20] | **Dip coating**[16, 21] | **3D printing**[4, 23] | **Bubble casting**[5] | **Flow casting** |
|---|---|---|---|---|---|
| Geometry complexity | 1D/2D | 3D | 3D | 1D/2D | 3D |
| Fabrication duration | Several hours | 1-2 days | Several hours | Several hours | Several hours |
| Mold piece(s) | Three or more | One | N/A | Two | One |
| Mold reusable | Yes | No | Yes | Yes | Yes |
| Mass-production available | Yes | Yes | No | Yes | Yes |

**Movie S1.** Fabrication process of flow casting. This video shows the fabrication process of a dyed soft tube (Ecoflex 0050). the precursor was first injected into the acrylic tube and then flowed out. Later, the casted layer was cured at room temperature. Finally, the cured soft tube was demolding out of the acrylic tube by a peel-dominated process.

**Movie S2.** Demolding processes of flow-cast soft tubes. This video shows the demolding processes of two soft tubes made of Ecoflex 0050 and a mixture (mass ratio of Ecoflex 0030: Dragon skin 30 = 1:2). The higher modulus soft shell (the mixture) resulted in a quicker and more fluent demolding process.

**Movie S3.** Demonstration of the soft vascular replica for a small magnetic robot transporting. This video shows that a small-scale magnetic robot navigates through the soft vascular replica by a manually controlled permanent magnet.

**Movie S4.** Demonstration of the soft sleeves for grasping enhancement. This video shows the rigid gripper failed to hold a 200 g weight with a smooth surface and a gel ball with a slippery surface. By wearing soft sleeves, the rigid gripper with soft sleeves succeeds in holding the 200 g weight, the gel ball, and other items, including a cherry tomato, a screw, a test tube, and a flesh driver.

**Movie S5.** Demonstration of the soft waveguide for color changing. The output colors shift to cyan, purple, and greenish yellow when the branches of red, green, and blue LEDs are stretched, respectively.